Locally adaptive density estimation on Riemannian Manifolds.

Guillermo Henry[1,2], Andrés Muñoz[1] and Daniela Rodriguez[1,2]
[1]*Facultad de Ciencias Exactas y Naturales, Universidad de Buenos Aires and* [1]*CONICET, Argentina.*

Abstract

In this paper, we consider a kernel type estimator with variable bandwidth when the random variables belong in a Riemannian manifolds. We study asymptotic properties such as the consistency and the asymptotic distribution. A simulation study is also consider to evaluate the performance of the proposal. Finally, to illustrate the potential applications of the proposed estimator, we analyzed two real example where two different manifolds are considered.

Key words and phrases: Asymptotic results, Density estimation, Meteorological applications, Nonparametric, Palaeomagnetic data, Riemannian manifolds.

1 Introduction

Let $X_1, \ldots, X_n$ be independent and identically distributed random variables taking values in $\mathbb{R}^d$ and having density function f. A class of estimators of f which has been widely studied since the work of Rosenblatt (1956) and Parzen (1962) in the univariate case ($d = 1$) and Silverman (1986) in the multidimensional setting, has the form

$$f_n(x) = \frac{1}{nh^d} \sum_{j=1}^{n} K\left(\frac{x - X_j}{h}\right),$$

where $K(u)$ is a bounded density on $\mathbb{R}^d$ and h is a sequence of positive numbers such that $h \to 0$ and $nh^d \to \infty$ as $n \to \infty$. Note that in this case, we consider a single smoothing parameter in all directions, however a more general form can be consider with a bandwidth matrix, for more details see Silverman (1986).

If we apply this estimator to data coming from long tailed distributions, with a small enough h to appropriate for the central part of the distribution, a spurious noise appears in the tails. With a large value of h for correctly handling the tails, we can not see the details occurring in the main part of the distribution. To overcome these defects, adaptive kernel estimators were introduced. For instance, a conceptually similar estimator of $f(x)$ was studied by Wagner (1975) who defined a general neighbor density estimator by

$$\widehat{f}_n(x) = \frac{1}{nH_n^d(x)} \sum_{j=1}^{n} K\left(\frac{x - X_j}{H_n(x)}\right),$$

where $k = k_n$ is a sequence of non–random integers such that $\lim_{n\to\infty} k_n = \infty$, and $H_n(x)$ is the distance between x and its k-nearest neighbor among $X_1, \ldots, X_n$, more precisely, $H_n(x)$ is the radius of the sphere centered at x and containing at least k of $X_1, \ldots, X_n$. Through these adaptive bandwidth , the estimation in the point x has the guarantee that to be calculated using at least k points of the sample.

However, in many applications, the variables X take values on different spaces than $\mathbb{R}^d$. Usually these spaces have a more complicated geometry than the Euclidean space and this has to be taken into account in the analysis of the data. For example if we study the distribution of the stars with luminosity in a given range it is naturally to think that the variables belong to a spherical cylinder ($S^2 \times \mathbb{R}$) instead of $\mathbb{R}^4$. If we consider a region of the planet M, then the direction and the velocity of the wind in this region are points in the tangent bundle of M, that is a manifold of dimension 4. Other examples could be found in image analysis, mechanics, geology and other fields. They include distributions on spheres, Lie groups, among others. See for example Joshi, et.at. (2007), Goh and Vidal (2008). For this reason, it is interesting to study an estimation procedure of the density function that take into account a more complex structure of the variables.

Nonparametric kernel methods for estimating densities of spherical data have been studied by Hall, et .al (1987) and Bai, et. al. (1988). Pelletier (2005) proposed a family of nonparametric estimators for the density function based on kernel weight when the variables are random object valued in a closed Riemannian manifold. The Pelletier's estimators is consistent with the kernel density estimators in the Euclidean, i.e., it coincides to the kernel estimator considered by Rosenblatt (1956) and Parzen (1962) when the manifold is $\mathbb{R}^d$.

As we comment above, the importance of consider a local adaptive bandwidth is well known in nonparametric statistics and this is even more true with data taking values on complexity space. This fact is due to the local structure of the manifolds, where the neighborhood of each point changes its shape due the curvature of the manifold. In this paper, we propose a kernel density estimate on a Riemannian manifold with a variable bandwidth defined by k-nearest neighbors.

This paper is organized as follows. Section 2 contains a brief summary of the necessaries concepts of Riemannian geometry. In Section 2.1, we introduce the estimator. Uniform consistency of the estimators is derived in Section 3.1, while in Section 3.2 the asymptotic distribution is obtained under regular assumptions. Section 4 contains a Monte Carlo study designed to evaluate the proposed estimators. Finally, Section 5 presents two example using real data. Proofs are given in the Appendix.

2 Preliminaries and the estimator

Let (M, g) be a $d-$dimensional Riemannian manifold without boundary. We denote by d_g the distance induced by the metric g. Throughout this paper we will asumme that (M, g) is a complete Riemannian manifold, i.e. (M, d_g) is a complete metric space. If $p \in M$, let $B_s(0_p)$ be the set of tangent vectors of p with norm less than s. An open neighbor $B_s(p)$ of p is called a normal ball of radius s centered at p if the exponential

map $exp_p|_{B_s(0_p)} : B_s(0_p) \longrightarrow B_s(p)$ is a diffeomorphism. The injectivity radius of (M, g) is defined by

$$inj_g M = \inf_{p \in M} \sup\{s \in I\!R > 0 : B_s(p) \text{ is a normal ball}\}.$$

Therefore if $s \leq inj_g M$ there is a normal ball of radius s centered at any p in M. In order to ensure the existence of a normal ball with fixed radius $s_0 > 0$ centered at any point of the manifold we will assume that the injectivity radius is positive.

Let $p \in M$ and $\{v_1, \ldots, v_d\}$ be an orthonormal basis of T_pM and consider the linear map $\xi : I\!R^d \longrightarrow T_pM$ defined by $\xi(a_1, \ldots, a_n) = \sum_{i=1}^d a_i v_i$. If $B_s(p)$ is a normal ball, we can defined $(B_s(p), \psi)$, a normal chart at p where $\psi : B_s(p) \longrightarrow I\!R^d$ and $\psi(q) = \xi^{-1} \circ exp_p^{-1}(q)$. Let (B_{s_0}, ψ) be a normal chart at p whit $s_0 = inj_g$, if $q \in B_{s_0}(p)$ consider the matrix $[g(q)]_{ij} = g(q)(\frac{\partial}{\partial \psi_i}\Big|_q, \frac{\partial}{\partial \psi_j}\Big|_q)$, where $\{\frac{\partial}{\partial \psi_i}|_q\}_{i=1}^d$ is the base of T_qM induced by $(B_{s_0}(p), \psi)$. We define $\theta_p : M \longrightarrow I\!R_{>0}$ by

$$\theta_p(q) = \begin{cases} \Big(\det[g(q)]\Big)^{\frac{1}{2}} & \text{if} \quad q \in B_{s_0}(p) \\ 1 & \text{if} \quad q \notin B_{s_0}(p) \end{cases}$$

The map θ_p is called the volume density function. It is not difficult to see that θ_p not depends on the election of the base $\{v_1, \ldots, v_d\}$. See Besse (1978), Pennec (2006) and Henry and Rodriguez (2009) for a more detailed discussion about this function. We finish the section showing some examples.

i) For the Euclidean space $(I\!R^d, g_0)$ the density function is $\theta_p(q) = 1$. Also for the cylinder of radius 1 endowed with the metric induced by the canonical metric of $I\!R^3$, the volume density function if constantly equal to 1.

ii) For the 2-dimensional sphere of radius R, the volume density function is

$$\theta_{p_1}(p_2) = R\,\frac{\sin(d_g(p_1, p_2)/R)}{d_g(p_1, p_2)} \qquad \text{if } p_2 \neq p_1, -p_1 \;\text{ and } \theta_{p_1}(p_1) = \theta_{p_1}(-p_1) = 1.$$

where $d_g(p_1, p_2) = R \arccos(\frac{< p_1, p_2 >}{R^2})$.

2.1 The estimator

Consider a probability distribution with a density f on a complete $d-$dimensional Riemannian manifold (M, g) with positivy injectivity radius. Let $X_1, \ldots, X_n$ be i.i.d random object takes values on M with density f. A natural extension of the estimator proposed by Wagner (1975) in the context of a Riemannian manifold is to consider the following estimator

$$\widehat{f}_n(p) = \frac{1}{nH_n^d(p)} \sum_{j=1}^n \frac{1}{\theta_{X_j}(p)} K\left(\frac{d_g(p, X_j)}{H_n(p)}\right),$$

where $K : I\!R \to I\!R$ is a non-negative function, $\theta_p(q)$ denotes the volume density function on (M, g) and $H_n(p)$ is the distance d_g between p and the k-nearest neighbor of p among $X_1, \ldots, X_n$, and $k = k_n$ is a sequence of non–random integers such that $\lim_{n\to\infty} k_n = \infty$.

We consider a kernel K with compact support and the bandwidth $\zeta_n(p) = \min\{H_n(p), inj_g M\}$ instead of $H_n(p)$. Thus, the kernel only takes in account the points X_i such that $d_g(X_i, p) \leq \zeta_n(p) \leq inj_g M$. In that points $\theta_p(X_i)$ is the volume of the parallelepiped spanned by the canonical tangent vectors $\{\frac{\partial}{\partial\psi_i}|_{X_i}\}_{j=1}^d$ induced by the normal chart $(B_s(p), \psi)$ with $s = inj_g M$. Hence, the $k-$nearest neighbor kernel type estimator is defined as follows,

$$\widehat{f}_n(p) = \frac{1}{n\zeta_n^d(p)} \sum_{j=1}^{n} \frac{1}{\theta_{X_j}(p)} K\left(\frac{d_g(p, X_j)}{\zeta_n(p)}\right), \tag{1}$$

Remark 2.1.1. If (M, g) is a compact Riemannian manifold it is not difficult to see that $inj_g M > 0$. In adition if the sectional curvature is not larger than $a > 0$, then $inj_g M \geq min\{\pi/\sqrt{a}, l/2\}$ where l is the length of the shortest closed geodesic in (M, g) (see Gallot, Hulin, Lafontaine (2004)).

3 Asymptotic results

Denote by $C^\ell(U)$ the set of ℓ times continuously differentiable functions from U to $I\!R$ where U is an open set of M. We assume that the measure induced by the probability P and by X is absolutely continuous with respect to the Riemannian volume measure $d\nu_g$, and we denote by f its density on M with respect to $d\nu_g$. More precisely, let $\mathcal{B}(M)$ be the Borel $\sigma-$field of M (the $\sigma-$field generated by the class of open sets of M). The random variable X has a probability density function f, i.e. if $\chi \in \mathcal{B}(M)$, $P(X^{-1}(\chi)) = \int_\chi f d\nu_g$.

3.1 Uniform Consistency

We will consider the following set of assumptions in order to derive the strong consistency results of the estimate $\widehat{f}_n(p)$ defined in (1).

*H*1. Let M_0 be a compact set on M such that:

i) f is a bounded function such that $\inf_{p\in M_0} f(p) = A > 0$.

ii) $\inf_{p,q\in M_0} \theta_p(q) = B > 0$.

*H*2. For any open set U_0 of M_0 such that $M_0 \subset U_0$, f is of class C^2 on U_0.

*H*3. The sequence k_n is such that $k_n \to \infty$, $\frac{k_n}{n} \to 0$ and $\frac{k_n}{\log n} \to \infty$ as $n \to \infty$.

*H*4. $K : I\!R \to I\!R$ is a bounded nonnegative Lipschitz function of order one, with compact support $[0, 1]$ satisfying: $\int_{I\!R^d} K(\|\mathbf{u}\|)d\mathbf{u} = 1$, $\int_{I\!R^d} \mathbf{u}K(\|\mathbf{u}\|)d\mathbf{u} = \mathbf{0}$ and $0 < \int_{I\!R^d} \|\mathbf{u}\|^2 K(\|\mathbf{u}\|)d\mathbf{u} < \infty$.

$H5$. The kernel $K(u)$ verifies $K(uz) \geq K(z)$ for all $u \in (0,1)$.

Remark 3.1.1. The fact that $\theta_p(p) = 1$ for all $p \in M$ guarantees that $H1$ ii) holds. The assumption $H3$ is usual when dealing with nearest neighbor and the assumption $H4$ is standard when dealing with kernel estimators.

Theorem 3.1.2. Assume that $H1$ to $H5$ holds, then we have that

$$\sup_{p \in M_0} |\widehat{f}_n(p) - f(p)| \xrightarrow{a.s.} 0.$$

3.2 Asymptotic normality

To derive the asymptotic distribution of the proposed estimate, we will need two additional assumptions. We will denote with $\mathcal{V}_r$ the Euclidean ball of radius r centered at the origin and with $\lambda(\mathcal{V}_r)$ its Lebesgue measure.

$H5$. $f(p) > 0$, $f \in C^2(V)$ with $V \subset M$ an open neighborhood of M and the second derivative of f is bounded.

$H6$. The sequence k_n is such that $k_n \to \infty$, $k_n/n \to 0$ as $n \to \infty$ and there exists $0 \leq \beta < \infty$ such that $\sqrt{k_n n^{-4/(d+4)}} \to \beta$ as $n \to \infty$.

$H7$. The kernel verifies

i) $\int K_1(\|\mathbf{u}\|)\|\mathbf{u}\|^2 d\mathbf{u} < \infty$ where $K_1(\mathbf{u}) = K'(\|\mathbf{u}\|)\|\mathbf{u}\|$.

ii) $\|\mathbf{u}\|^{d+1} K_2(\mathbf{u}) \to 0$ as $\|\mathbf{u}\| \to \infty$ where $K_2(\mathbf{u}) = K''(\|\mathbf{u}\|)\|\mathbf{u}\|^2 - K_1(\mathbf{u})$.

Remark 3.2.1. Note that $div(K(\|\mathbf{u}\|)\mathbf{u}) = K'(\|\mathbf{u}\|)\|\mathbf{u}\| + d\ K(\|\mathbf{u}\|)$, then using the divergence Theorem, we get that $\int K'(\|\mathbf{u}\|)\|\mathbf{u}\| d\mathbf{u} = \int_{\|\mathbf{u}\|=1} K(\|\mathbf{u}\|)\mathbf{u}\frac{\mathbf{u}}{\|\mathbf{u}\|} d\mathbf{u} - d \int K(\|\mathbf{u}\|) d\mathbf{u}$. Thus, the fact that K has compact support in $[0,1]$ implies that $\int K_1(\mathbf{u}) d\mathbf{u} = -d$.

On the other hand, note that $\nabla(K(\|\mathbf{u}\|)\|\mathbf{u}\|^2) = K_1(\|\mathbf{u}\|)\mathbf{u} + 2K(\|\mathbf{u}\|)\mathbf{u}$ and by $H4$ we get that $\int K_1(\|\mathbf{u}\|)\mathbf{u} d\mathbf{u} = \mathbf{0}$.

Theorem 3.2.2. Assume $H4$ to $H7$. Then we have that

$$\sqrt{k_n}(\widehat{f}_n(p) - f(p)) \xrightarrow{\mathcal{D}} \mathcal{N}(b(p), \sigma^2(p))$$

with

$$b(p) = \frac{1}{2} \frac{\beta^{\frac{d+4}{d}}}{(f(p)\lambda(\mathcal{V}_1))^{\frac{2}{d}}} \int_{\mathcal{V}_1} K(\|\mathbf{u}\|) u_1^2 \, d\mathbf{u} \sum_{i=1}^{d} \frac{\partial f \circ \psi^{-1}}{\partial u_i \partial u_i}|_{u=0}$$

and

$$\sigma^2(p) = \lambda(\mathcal{V}_1) f^2(p) \int_{\mathcal{V}_1} K^2(\|\mathbf{u}\|) d\mathbf{u}$$

where $\mathbf{u} = (u_1, \ldots, u_d)$, $(B_h(p), \psi)$ is any normal chart and β is defined in assumption $H6$.

In order to derive the asymptotic distribution of $\widehat{f}_n(p)$, we will study the asymptotic behavior of $h_n^d/\zeta_n^d(p)$ where $h_n^d = k_n/(nf(p)\lambda(\mathcal{V}_1))$. Note that if we consider $\widetilde{f}_n(p) = k_n/(n\zeta_n^d(p)\lambda(\mathcal{V}_1))$, $\widetilde{f}_n(p)$ is a consistent estimator of $f(p)$ (see the proof of Theorem 3.1.2.). The next Theorem states that this estimator is also asymptotically normally distributed as in the Euclidean case.

Theorem 3.2.3. *Assume H4 to H6, and let $h_n^d = k_n/(nf(p)\lambda(\mathcal{V}_1))$. Then we have that*

$$\sqrt{k_n}\left(\frac{h_n^d}{\zeta_n^d(p)} - 1\right) \xrightarrow{\mathcal{D}} N(b_1(p), 1)$$

with

$$b_1(p) = \left(\frac{\beta^{\frac{d+4}{2}}}{f(p)\mu(\mathcal{V}_1)}\right)^{\frac{2}{d}} \left\{\frac{\tau}{6d+12} + \frac{\int_{\mathcal{V}_1} u_1^2\, d\mathbf{u}\; L_1(p)}{f(p)\mu(\mathcal{V}_1)}\right\}$$

where $\mathbf{u} = (u_1, \ldots, u_d)$, τ is the scalar curvature of (M, g), i.e. the trace of the Ricci tensor,

$$L_1(p) = \sum_{i=1}^{d}\left(\frac{\partial^2 f \circ \psi^{-1}}{\partial u_i u_i}\Big|_{u=0} + \frac{\partial f \circ \psi^{-1}}{\partial u_i}\Big|_{u=0} \frac{\partial \theta_p \circ \psi^{-1}}{\partial u_i}\Big|_{u=0}\right)$$

and $(B_h(p), \psi)$ is any normal chart.

Remark 3.2.4. Note that Theorems 3.1.2. and 3.2.2 generalize the asymptotic results obtained in Henry and Rodriguez (2009) for non variable bandwidth. The uniform consistency for both estimators is obtained under similar assumptions. More precisely, the assumptions $H1$, $H2$ and $H4$ are the same for both estimators and an equivalent condition to $H3$ is required for the bandwidth in Henry and Rodriguez (2009). The result related to the asymptotic normality is also similar for both estimators. In particular, if we choose the number of neighbor as $k_n = (nf(p)\lambda(\mathcal{V}_1))/h_n^d$, Theorem 3.2.2. can be derived heuristically from Theorem 4.1 in Henry and Rodriguez (2009).

4 Simulations

This section contains the results of a simulation study designed to evaluate the performance of the estimator defined in the Section 2.1. We consider four models in two different Riemannian manifolds, the sphere and the cylinder endowed with the metric induced by the canonical metric of $\mathbb{R}^3$. We performed 1000 replications of independent samples of sizes $n = 100$, 150 and 200 according to the following models:

Model 1 (in the sphere): The random variables X_i for $1 \leq i \leq n$ are i.i.d. Von Mises distribution $VM(\mu, \kappa)$ i.e.

$$f_{\mu,\kappa}(X) = \left(\frac{k}{2}\right)^{1/2} I_{1/2}(\kappa) \exp\{\kappa\, X^{\mathrm{T}}\boldsymbol{\mu}\},$$

with $\boldsymbol{\mu}$ is the mean parameter, $\kappa > 0$ is the concentration parameter and $I_{1/2}(\kappa) = \left(\frac{\kappa\pi}{2}\right)\sinh(\kappa)$ stands for the modified Bessel function. This model has many important applications, as described in Jammalamadaka and SenGupta (2001) and Mardia and Jupp (2000). We generate a random sample follows a Von Mises distribution with mean $(0, 0, 1)$ and concentration parameter 3.

Model 2 (in the sphere): We simulate i.i.d. random variables Z_i for $1 \leq i \leq n$ following a multivariate normal distribution of dimension 3, with mean $(0, 0, 0)$ and covariance matrix equals to the identity. We define $X_i = \frac{Z_i}{\|Z_i\|}$ for $1 \leq i \leq n$, therefore the variables X_i follow an uniform distribution in the two dimensional sphere. Note that this distribution is the projected normal distribution with mean $(0, 0, 0)$ and covarianza matrix equals to the identity.

Model 3 (in the cylinder): We consider random variables $X_i = (\mathbf{y}_i, t_i)$ taking values in the cylinder $S^1 \times I\!R$. We generated the model proposed by Mardia and Sutton (1978) where,

$$\mathbf{y}_i = (\cos(\theta_i), \sin(\theta_i)) \sim VM((-1, 0), 5)$$

$$t_i|\mathbf{y}_i \sim N(1 + 2\sqrt{5}\cos(\theta_i), 1).$$

Some examples of variables with this distribution can be found in Mardia and Sutton (1978).

Model 4 (in the cylinder): We generate random variables $X_i = (\mathbf{y}_i, t_i)$ taking values in the cylinder $S^1 \times I\!R$. We generated a truncated model where,

$$\mathbf{y}_i = (\cos(\theta_i), \sin(\theta_i)) \sim VM((-1, 0), 5)$$

$$t_i|\mathbf{y}_i \sim N(1 + 2\sqrt{5}\cos(\theta_i), 1).$$

and the variable t_i was truncated conditionally to $\mathbf{y}_i$, so that $t_i > 1 + 2\sqrt{5}\cos(\theta_i)$.

In all cases, for smoothing procedure, the kernel was taken as the quadratic kernel $K(t) = (15/16)(1 - t^2)^2 I_{(|t|<1)}$ where I_A denote the indicator function on the set A. We have considered a grid of equidistant values of k between 5 and 150 of length 20. Also when the sample size is $n = 100$, we added 20 neighbors more in the following grid $5 + 2k$ with $k = 0, 1, \ldots, 7$ and $24 + 5j$ and $50 + 10j$ for $j = 0, \ldots, 5$.

To study the performance of the estimators of the density function f, denoted by $\widehat{f}_n$, we have considered the mean square error (MSE) and the median square error (MedSE), i.e,

$$\text{MSE}(\widehat{f}_n) = \frac{1}{n}\sum_{i=1}^{n}[\widehat{f}_n(X_i) - f(X_i)]^2 \, .$$

$$\text{MedSE}(\widehat{f}_n) = \text{median}\,|\widehat{f}_n(X_i) - f(X_i)|^2 \, .$$

Figure 1 gives the values of the MSE and MedSE of $\widehat{f}_n$ for the models in the sphere considering different numbers of neighbors and sample sizes, while Figure 2 shows the cylinder

models. More precisely, for each number of neighbor and sample size, we summarize the results through the average of MSE and MedSE over the 1000 replications. In order to compare the performance of our estimator with the estimator with fixed bandwidth introduced in Pelletier (2005), we compute the Pelletier's estimator for the Models 1 and 2. Figure 3 summarizes the errors obtained for the Model 1 and 2 using the nonparametric estimator with non locally smoothing parameter for a grid of 20 bandwidths between 0.01 and 3.2. The comparison was compute for $n = 200$.

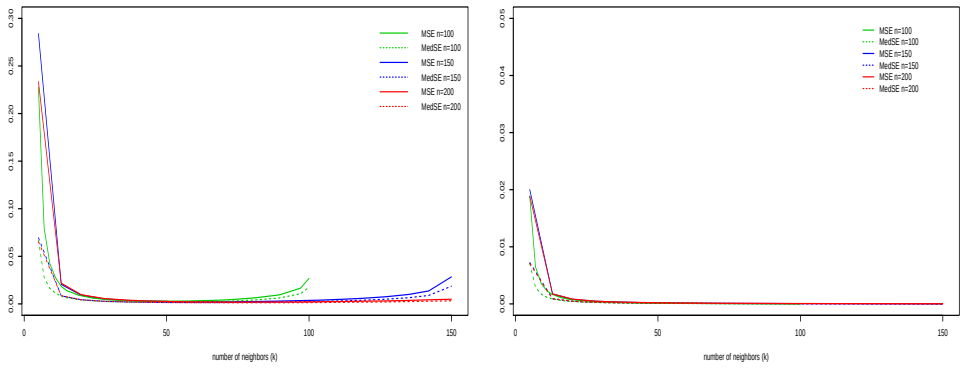

a) *b)*

Figure 1: Plot of the average of the errors using different numbers of neighbor for the models in the sphere, a) Model 1 and b) Model 2. The solid line corresponds to the Mean square error, while the dashed lines corresponds to the median square error. The colors correspond the different sample sizes green, blue and red for $n = 100, 150$ and 200, respectively.

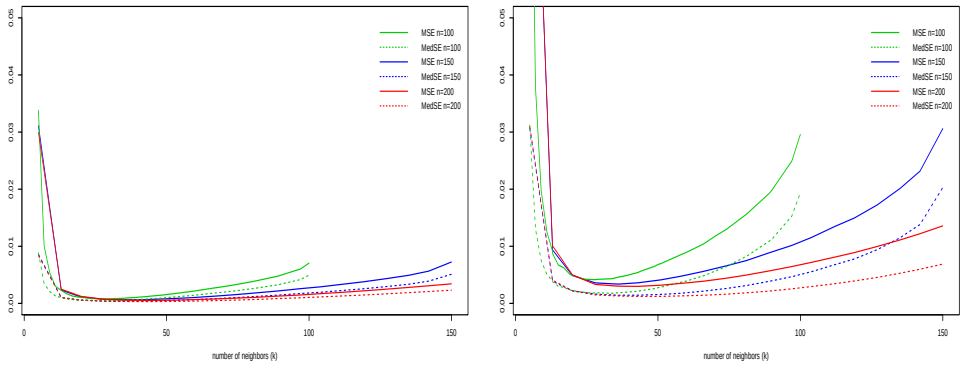

a) *b)*

Figure 2: Plot of the average of of the errors using different numbers of neighbor for the models in the cylinder, a) Model 3 and b) Model 4. The solid line corresponds to the Mean square error, while the dashed lines corresponds to the median square error. The colors correspond the different sample sizes green, blue and red for $n = 100, 150$ and 200, respectively.

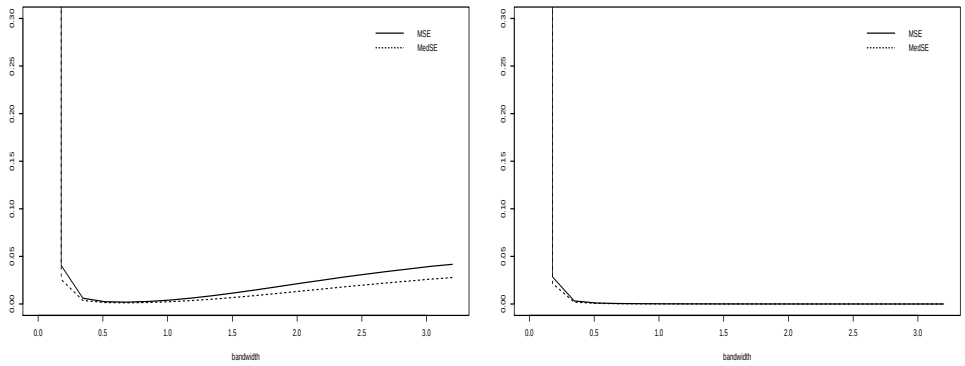

a) *b)*

Figure 3: Plot of the average of of the errors for the estimator in Model 1 and Model 2 using fixed smoothing parameter and sample size 200. The solid line corresponds to the Mean square error, while the dashed lines corresponds to the median square error over different values of bandwidth.

The simulation study confirms the good behavior of $k-$nearest neighbor estimators, under the different models considered. In all cases, the estimators are stable under large numbers of neighbors. However, as expected, the estimators using a small number of neighbors have a poor behavior, because in the neighborhood of each point there is a small number of samples. Also as we expected, the error decrease when the sample size increases.

In Figure 3, we can observe that the behavior for the estimator using the fixed and locally bandwidth are comparable. More precisely, in Model 1 the minimums of the average of the errors were 0.0019 and 0.001883 for fixed and variable bandwidth, respectively. Also, we compute the median of the average of the errors in each cases and we obtained 0.02 and 0.003 for fixed and variable bandwidth, respectively. In Model 2, we can conclude similarly. On the other hand for this model, we can observe that for both estimators, the errors decrease slightly for large values of neighbors or bandwidths. This fact is due to the uniform model, where the over smoothing tends to adjust well the model.

5 Real Example

5.1 Paleomagnetic data

It is well know the need for statistical analysis of paleomagnetic data. Since the work developed by Fisher (1953), the study of parametric families was considered a principal tool to analyze and quantify this type of data (see Cox and Doell (1960), Butler (1992) and Love and Constable (2003)). In particular, our proposal allows to explore the nature of directional dataset that include paleomagnetic data without making any parametric assumptions.

In order to illustrate the $k-$nearest neighbor kernel type estimator on the two-dimensional sphere, we illustrate the estimator using a paleomagnetic data set studied by Fisher, Lewis, and Embleton (1987). The data set consists in $n = 107$ sites from specimens of Precambrian volcanos whit measurements of magnetic remanence. The data set contains two variables

corresponding to the directional component on a longitude scale, and the directional component on a latitude scale. The original data set is available in the library sm of R statistical package.

To calculate the estimators the volume density function and the geodesic distance were taken as in the Section 2 and we considered the quadratic kernel $K(t) = (15/16)(1 - t^2)^2 I(|t| < 1)$. In order to analyzed the sensitivity of the results with respect to the number of neighbors, we plot the estimator using values of k. The results are shown in the Figure 4.

The real data was plotted in blue and with a large radius in order to obtain a better visualization. The Equator line, the Greenwich meridian and a second meridian are in gray while the north and south pols are denoted with the capital letter N and S respectively. The levels of concentration of measurements of magnetic remanence can be found in yellow for high levels and in red for lowest density levels. Also, the levels of concentration of measurements of magnetic remanence was illustrated with relief on the sphere that allow to emphasize high density levels and the form of the density function.

As in the Euclidean case large number of neighbors produce estimators with small variance but high bias, while small values produce more wiggly estimators. This fact shows the need of the implementation of a method to select the adequate bandwidth for this estimators. However, this require further careful investigation and are beyond the scope of this paper.

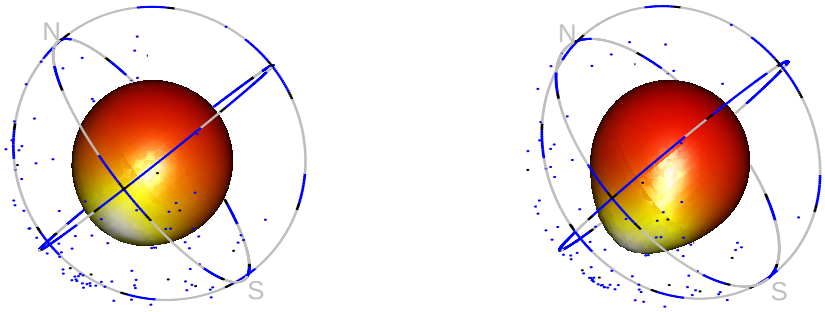

a) *b)*

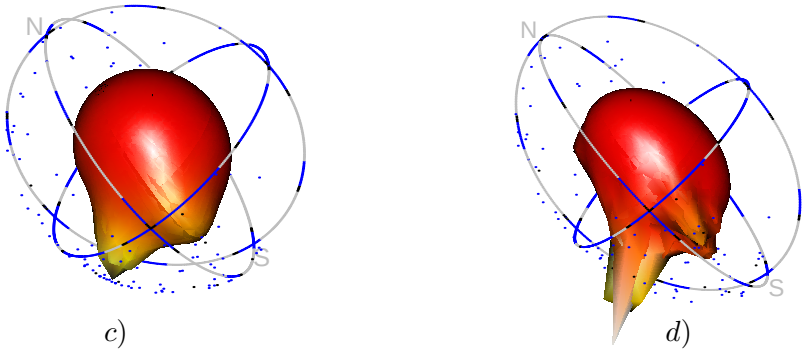

c) d)

Figure 4: The locally adaptive density estimator using different number of neighbors, a) $k = 75$, b)$k = 50$, c) $k = 25$ and d) $k = 10$.

5.2 Meteorological data

In this Section, we consider a real data set collected in the meteorological station "Agüita de Perdiz" that is located in Viedma, province of Río Negro, Argentine. The dataset consists in the wind direction and temperature during January 2011 and contains 1326 measurements that were registered with a frequency of thirty minutes. We note that the considered variables belong to a cylinder with radius 1.

As in the previous Section, we consider the quadratic kernel and we took the density function and the geodesic distance as in Section 2. Figure 5 shows the result of the estimators, the color and form of the graphic was constructed as in the previous example.

It is important to remark that the measurement devices of wind direction not present a sufficient precision to avoid repeated data. Therefore, we consider the proposal given in García-Portugués, et.al. (2011) to solve this problem. The proposal consists in perturb the repeated data as follows $\widetilde{r}_i = r_i + \xi\varepsilon_i$, where r_i denote the wind direction measurements and ε_i, for $i = 1, \ldots, n$ were independently generated from a von Mises distribution with $\mu = (1, 0)$ and $\kappa = 1$. The selection of the perturbation scale ξ was taken $\xi = n^{-1/5}$ as in García-Portugués, et.al. (2011) where in this case $n = 1326$.

The work of García-Portugués, et.al. (2011) contains other nice real example where the proposed estimator can be apply. They considered a naive density estimator applied to wind directions and SO2 concentrations, that allow you explore high levels of contamination.

In Figure 5, we can see that the lowest temperature are more probable when the wind comes from the East direction. However, the highest temperature does not seem to have correlation with the wind direction. Also, note that in Figure 4, we can see two mode corresponding to the minimum and maximum daily of the temperature.

These examples show the usefulness of the proposed estimator for the analysis and exploration of these type of dataset.

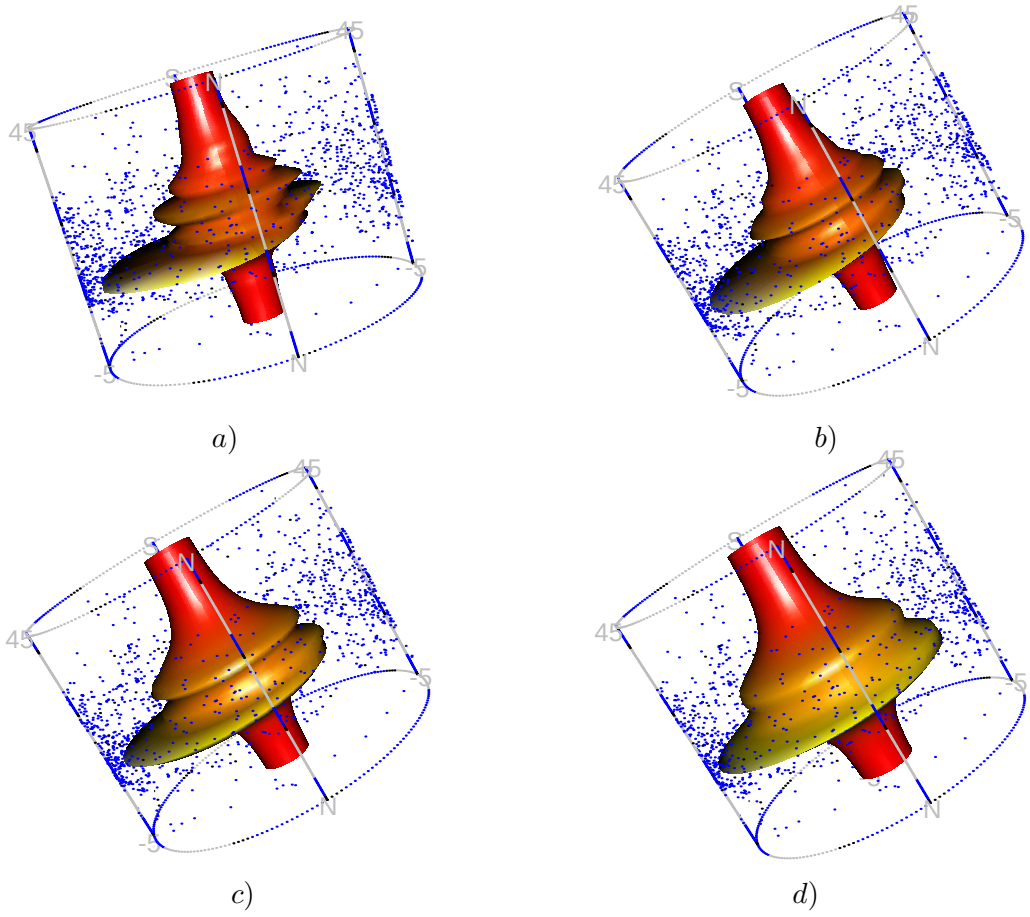

Figure 5: The locally adaptive density estimator using different number of neighbors, a) $k = 75$, b)$k = 150$, c) $k = 300$ and d) $k = 400$.

Appendix

Proof of Theorem 3.1.2.

Let

$$f_n(p, \delta_n) = \frac{1}{n\delta_n^d} \sum_{i=1}^{n} \frac{1}{\theta_{X_i}(p)} K\left(\frac{d_g(p, X_i)}{\delta_n}\right) .$$

Note that $\widehat{f}_n(p) = f_n(p, \zeta_n(p))$, and if $\delta_n = \zeta_n(p)$ verifies $\delta_{1n} \leq \zeta_n(p) \leq \delta_{2n}$ for all $p \in M_0$ where δ_{1n} and δ_{2n} satisfy $\delta_{in} \to 0$ and $\dfrac{n\delta_{in}^d}{\log n} \to \infty$ as $n \to \infty$ for $i = 1, 2$ then by Theorem

3.2 in Henry and Rodriguez (2009) we have that

$$\sup_{p\in M_0} |f_n(p,\delta_n) - f(p)| \xrightarrow{a.s.} 0 \tag{2}$$

For each $0<\beta<1$ we define,

$$f_n^-(p,\beta) = \frac{1}{nD_n^+(\beta)^d}\sum_{i=1}^n \frac{1}{\theta_{X_i}(p)} K\left(\frac{d_g(p,X_i)}{D_n^-(\beta)}\right) = f_n^-(p, D_n^-(\beta)^d)\frac{D_n^-(\beta)^d}{D_n^+(\beta)^d}\,.$$

$$f_n^+(p,\beta) = \frac{1}{nD_n^-(\beta)^d}\sum_{i=1}^n \frac{1}{\theta_{X_i}(p)} K\left(\frac{d_g(p,X_i)}{D_n^+(\beta)}\right) = f_n^+(p, D_n^+(\beta)^d)\frac{D_n^+(\beta)^d}{D_n^-(\beta)^d}\,.$$

where $D_n^-(\beta) = \beta^{1/2d}h_n$, $D_n^+(\beta) = \beta^{-1/2d}h_n$ and $h_n^d = k_n/(n\lambda(\mathcal{V}_1)f(p))$ with $\lambda(\mathcal{V}_1)$ denote the Lebesgue measure of the ball in $\mathbb{R}^d$ with radius r centered at the origin. Note that

$$\sup_{p\in M_0} |f_n^-(p,\beta) - \beta f(p)| \xrightarrow{a.s.} 0 \text{ and } \sup_{p\in M_0} |f_n^+(p,\beta) - \beta^{-1} f(p)| \xrightarrow{a.s.} 0. \tag{3}$$

For all $0<\beta<1$ and $\varepsilon>0$ we define

$$\begin{aligned}
S_n^-(\beta,\varepsilon) &= \{w : \sup_{p\in M_0} |f_n^-(p,\beta) - f(p)| < \varepsilon\,\},\\
S_n^+(\beta,\varepsilon) &= \{w : \sup_{p\in M_0} |f_n^+(p,\beta) - f(p)| < \varepsilon\,\},\\
S_n(\varepsilon) &= \{w : \sup_{p\in M_0} |\widehat{f}_n(p) - f(p)| < \varepsilon\,\},\\
A_n(\beta) &= \{f_n^-(p,\beta) \le \widehat{f}_n(p) \le f_n^+(p,\beta)\}.
\end{aligned}$$

Then, $A_n(\beta)\cap S_n^-(\beta,\varepsilon)\cap S_n^+(\beta,\varepsilon)\subset S_n(\varepsilon)$. Let $A = \sup_{p\in M_0} f(p)$. For $0<\varepsilon<3A/2$ and $\beta_\varepsilon = 1-\frac{\varepsilon}{3A}$ consider the following sets

$$\begin{aligned}
G_n(\varepsilon) &= \{w :\ D_n^-(\beta_\varepsilon) \le \zeta_n(p) \le D_n^+(\beta_\varepsilon) \ \text{ for all } p\in M_0\}\\
G_n^-(\varepsilon) &= \{\sup_{p\in M_0} |f_n^-(p,\beta_\varepsilon) - \beta_\varepsilon f(p)| < \frac{\varepsilon}{3}\}\\
G_n^+(\varepsilon) &= \{\sup_{p\in M_0} |f_n^+(p,\beta_\varepsilon) - \beta_\varepsilon^{-1} f(p)| < \frac{\varepsilon}{3}\}.
\end{aligned}$$

Then we have that $G_n(\varepsilon)\subset A_n(\beta_\varepsilon)$, $G_n^-(\varepsilon)\subset S_n^-(\beta_\varepsilon,\varepsilon)$ and $G_n^+(\varepsilon)\subset S_n^+(\beta_\varepsilon,\varepsilon)$. Therefore, $G_n(\varepsilon)\cap G_n^-(\varepsilon)\cap G_n^+(\varepsilon)\subset S_n(\varepsilon)$.

On the other hand, using that $\lim_{r\to 0} V(B_r(p))/r^d\mu(\mathcal{V}_1) = 1$, where $V(B_r(p))$ denotes the volume of the geodesic ball centered at p with radius r (see Gray and Vanhecke (1979)) and similar arguments those considered in Devroye and Wagner (1977), we get that

$$\sup_{p\in M_0}\left|\frac{k_n}{n\lambda(\mathcal{V}_1)f(p)H_n^d(p)} - 1\right| \xrightarrow{a.s.} 0. \tag{4}$$

Recall that $inj_g M > 0$ and $H_n^d(p) \xrightarrow{a.s.} 0$, since (4), $k_n/n\to 0$ and $H1$ i). Then for straightforward calculations we obtained that $\sup_{p\in M_0}\left|\frac{k_n}{n\lambda(\mathcal{V}_1)f(p)\zeta_n^d(p)} - 1\right| \xrightarrow{a.s.} 0$. Thus if we denote I_A de indicator function on the set A, , $I_{G_n^c(\varepsilon)} \xrightarrow{a.s.} 0$ and (3) imply that $I_{S_n^c(\varepsilon)} \xrightarrow{a.s.} 0$. □

Proof of Theorem 3.2.2.

A Taylor expansion of second order gives

$$\sqrt{k_n}\left\{\frac{1}{n\zeta_n^d(p)}\sum_{j=1}^{n}\frac{1}{\theta_{X_j}(p)}K\left(\frac{d_g(p,X_j)}{\zeta_n(p)}\right)-f(p)\right\}=A_n+B_n+C_n$$

where

$$\begin{aligned}
A_n &= (h_n^d/\zeta_n^d(p))\sqrt{k_n}\left\{\frac{1}{nh_n^d}\sum_{j=1}^{n}\frac{1}{\theta_{X_j}(p)}K\left(\frac{d_g(p,X_j)}{h_n}\right)-f(p)\right\},\\
B_n &= \sqrt{k_n}((h_n^d/\zeta_n^d(p))-1)\left\{f(p)+\frac{[(h_n/\zeta_n(p))-1]h_n^d}{[(h_n^d/\zeta_n^d(p))-1]\zeta_n^d(p)}\ \frac{1}{nh_n^d}\sum_{j=1}^{n}\frac{1}{\theta_{X_j}(p)}K_1\left(\frac{d_g(p,X_j)}{\zeta_n(p)}\right)\right\}
\end{aligned}$$

and

$$C_n = \sqrt{k_n}((h_n^d/\zeta_n^d(p))-1)\frac{[(h_n/\zeta_n(p))-1]^2}{2[(h_n^d/\zeta_n^d(p))-1]}\ \frac{1}{n\zeta_n^d(p)}\sum_{j=1}^{n}\frac{1}{\theta_{X_j}(p)}K_2\left(\frac{d_g(p,X_j)}{\xi_n}\right)[\xi_n/h_n]^2$$

with $h_n^d=k_n/nf(p)\lambda(\mathcal{V}_1)$; $\min(h_n,\zeta_n)\le\xi_n\le\max(h_n,\zeta_n)$ and K_1 and K_2 defined in $H7$. Note that $H6$ implies that h_n satisfies the necessary hypothesis given in Theorem 4.1 in Rodriguez and Henry (2009), in particular

$$\sqrt{nh_n^{d+4}}\to\beta^{\frac{d+4}{d}}(f(p)\lambda(\mathcal{V}_1))^{-\frac{d+4}{2d}}.$$

By the Theorem and the fact that $h_n/\zeta_n(p)\xrightarrow{p}1$, we obtain that A_n converges to a normal distribution with mean $b(p)$ and variance $\sigma^2(p)$. Therefore it is enough to show that B_n and C_n converges to zero in probability.

Note that $\frac{(h_n/H_n(p))-1}{(h_n^d/\zeta_n^d(p))-1}\xrightarrow{p}d^{-1}$ and by similar arguments those considered in Theorem 3.1 in Pelletier (2005) and Remark 3.2.1. we get that

$$\frac{1}{nh_n^d}\sum_{j=1}^{n}\frac{1}{\theta_{X_j}(p)}K_1\left(\frac{d_g(p,X_j)}{\zeta_n(p)}\right)\xrightarrow{p}\int K_1(\mathbf{u})d\mathbf{u}f(p)=-d\ f(p).$$

Therefore, by Theorem 3.2.3., we obtain that $B_n\xrightarrow{p}0$. As ξ_n/h_n converges to one in probability, in order to concluded the proof, it remains to prove that

$$\frac{1}{n\zeta_n^d(p)}\sum_{j=1}^{n}\frac{1}{\theta_{X_j}(p)}|K_2\left(d_g(p,X_j)/\xi_n\right)|$$

is bounded in probability.

By $H7$, there exits $r>0$ such that $|t|^{d+1}|K_2(t)|\le 1$ if $|t|\ge r$. Let $C_r=(-r,r)$, then we have that

$$\frac{1}{n\zeta_n^d(p)}\sum_{j=1}^{n}\frac{1}{\theta_{X_j}(p)}\left|K_2\left(\frac{d_g(p,X_j)}{\xi_n}\right)\right|\le\frac{\sup_{|t|\le r}|K_2(t)|}{n\zeta_n^d(p)}\sum_{j=1}^{n}\frac{1}{\theta_{X_j}(p)}I_{C_r}\left(\frac{d_g(p,X_j)}{\xi_n}\right)$$

$$+\frac{1}{n\zeta_n^d(p)}\sum_{j=1}^{n}\frac{1}{\theta_{X_j}(p)}I_{C_r^c}\Big(\frac{d_g(p,X_j)}{\xi_n}\Big)\Big|\frac{d_g(p,X_j)}{\xi_n}\Big|^{-(d+1)}$$

As $\min(h_n,\zeta_n(p))\leq\xi_n\leq\max(h_n,\zeta_n(p))=\widetilde{\xi}_n$ it follows that

$$\begin{aligned}
\frac{1}{n\zeta_n^d(p)} & \sum_{j=1}^{n}\frac{1}{\theta_{X_j}(p)}\left|K_2\left(\frac{d_g(p,X_j)}{\xi_n}\right)\right|\leq \\
&\leq \left(\frac{h_n}{\zeta_n(p)}\right)^d\sup_{|t|\leq r}|K_2(t)|\,\frac{1}{nh_n^d}\sum_{j=1}^{n}\frac{1}{\theta_{X_j}(p)}I_{C_r}\Big(\frac{d_g(p,X_j)}{h_n}\Big)\\
&+\sup_{|t|\leq r}|K_2(t)|\,\frac{1}{n\zeta_n^d(p)}\sum_{j=1}^{n}\frac{1}{\theta_{X_j}(p)}I_{C_r}\Big(\frac{d_g(p,X_j)}{\zeta_n(p)}\Big)\\
&+\left(\frac{h_n}{\zeta_n(p)}\right)^d\frac{1}{nh_n^d}\sum_{j=1}^{n}\frac{1}{\theta_{X_j}(p)}I_{C_r^c}\Big(\frac{d_g(p,X_j)}{h_n}\Big)\Big|\frac{d_g(p,X_j)}{h_n}\Big|^{-(d+1)}\Big|\frac{\widetilde{\xi}_n}{h_n}\Big|^{(d+1)}\\
&+\frac{1}{n\zeta_n^d(p)}\sum_{j=1}^{n}\frac{1}{\theta_{X_j}(p)}I_{C_r^c}\Big(\frac{d_g(p,X_j)}{\zeta_n(p)}\Big)\Big|\frac{d_g(p,X_j)}{\zeta_n(p)}\Big|^{-(d+1)}\Big|\frac{\widetilde{\xi}_n}{\zeta_n(p)}\Big|^{(d+1)}\\
&= C_{n1}+C_{n2}+C_{n3}+C_{n4}.
\end{aligned}$$

By similar arguments those considered in Theorem 5 in Boente and Fraiman (1991), we have that $C_{n1}\xrightarrow{p} f(p)\int I_{C_r}(s)ds$ and $C_{n3}\xrightarrow{p} f(p)\int I_{C_r^c}(s)|s|^{-(d+1)}ds$.

Finally, let $A_n^\varepsilon=\{(1-\varepsilon)h_n\leq\zeta_n\leq(1+\varepsilon)h_n\}$ for $0\leq\varepsilon\leq 1$. Then for n large enough $P(A_n^\varepsilon)>1-\varepsilon$ and in A_n^ε we have that

$$\begin{aligned}
I_{C_r}\left(\frac{d_g(X_j,p)}{\zeta_n(p)}\right) &\leq I_{C_r}\left(\frac{d_g(X_j,p)}{(1+\varepsilon)h_n}\right),\\
I_{C_r^c}\left(\frac{d_g(X_j,p)}{\zeta_n(p)}\right)\left|\frac{d_g(X_j,p)}{\zeta_n(p)}\right|^{-(d+1)} &\leq I_{C_r^c}\left(\frac{d_g(X_j,p)}{(1-\varepsilon)h_n}\right)\left|\frac{d_g(X_j,p)}{(1-\varepsilon)h_n}\right|^{-(d+1)}\left|\frac{\zeta_n(p)}{(1-\varepsilon)h_n}\right|^{(d+1)}.
\end{aligned}$$

This fact and analogous arguments those considered in Theorem 3.1 in Pelletier (2005), allow to conclude the proof.□

Proof of Theorem 3.2.3.

Denote $b_n=h_n^d/(1+zk_n^{-1/2})$, then

$$P(\sqrt{k_n}(h_n^d/\zeta_n^d-1)\leq z)=P(\zeta_n^d\geq b_n)=P(H_n^d\geq b_n,\ inj_gM^d\geq b_n).$$

As $b_n\to 0$ and $inj_gM>0$, there exists n_0 such that for all $n\geq n_0$ we have that

$$P(H_n^d\geq b_n,\ inj_gM^d\geq b_n)=P(H_n^d\geq b_n).$$

Let Z_i such that $Z_i = 1$ when $d_g(p, X_i) \leq b_n^{1/d}$ and $Z_i = 0$ elsewhere. Thus, we have that $P(H_n^d \geq b_n) = P(\sum_{i=1}^n Z_i \leq k_n)$. Let $q_n = P(d_g(p, X_i) \leq b_n^{1/d})$. Note that $q_n \to 0$ and $nq_n \to \infty$ as $n \to \infty$, therefore

$$P\left(\sum_{i=1}^n Z_i \leq k_n\right) = P\left(\frac{1}{\sqrt{nq_n}}\sum_{i=1}^n (Z_i - E(Z_i)) \leq \frac{1}{\sqrt{nq_n}}(k_n - nq_n)\right).$$

Using the Lindeberg Central Limit Theorem we easily obtain that $(nq_n)^{-1/2}\sum_{i=1}^n (Z_i - E(Z_i))$ is asymptotically normal with mean zero and variance one. Hence, it is enough to show that $(nq_n)^{-1/2}(k_n - nq_n) \xrightarrow{p} z + b_1(p)$.

Denote by $\mu_n = n \int_{B_{b_n^{1/d}}(p)} (f(q) - f(p)) d\nu_g(q)$. Note that $\mu_n = n\ q_n - w_n$ with $w_n = n\ f(p) V(B_{b_n^{1/d}}(p))$. Thus,

$$\frac{1}{\sqrt{nq_n}}(k_n - nq_n) = w_n^{-1/2}(k_n - w_n)\left(\frac{w_n}{w_n + \mu_n}\right)^{1/2} + \frac{\mu_n}{w_n^{1/2}}\left(\frac{w_n}{w_n + \mu_n}\right)^{1/2}.$$

Let $(B_{b_n^{1/d}}(p), \psi)$ be a coordinate normal system. Then, we note that

$$\frac{1}{\lambda(\mathcal{V}_{b_n^{1/d}})}\int_{B_{b_n^{1/d}}(p)} f(q) d\nu_g(q) = \frac{1}{\lambda(\mathcal{V}_{b_n^{1/d}})}\int_{\mathcal{V}_{b_n^{1/d}}} f \circ \psi^{-1}(\mathbf{u})\theta_p \circ \psi^{-1}(\mathbf{u}) d\mathbf{u}.$$

The Lebesgue's Differentiation Theorem and the fact that $\dfrac{V(B_{b_n^{1/d}}(p))}{\lambda(\mathcal{V}_{b_n^{1/d}})} \to 1$ imply that $\dfrac{\lambda_n}{w_n} \to 0$. On the other hand, from Gray and Vanhecke (1979), we have that

$$V(B_r(p)) = r^d \lambda(\mathcal{V}_1)(1 - \frac{\tau}{6d+12} r^2 + O(r^4)).$$

Hence, we obtain that

$$\begin{aligned} w_n^{-1/2}(k_n - w_n) &= \frac{w_n^{-1/2}\ k_n\ z\ k_n^{-1/2}}{1 + z k_n^{-1/2}} + \frac{w_n^{-1/2}\ \tau b_n^{2/d}\ k_n}{(6d+12)(1 + z k_n^{-1/2})} + w_n^{-1/2}\ k_n\ O(b_n^{4/d}) \\ &= A_n + B_n + C_n. \end{aligned}$$

It's easy to see that $A_n \to z$ and $w_n^{-1/2}\ b_n^{2/d}\ k_n = \frac{k_n n^{-1/2} b_n^{2/d - 1/2}}{(f(p)\lambda(\mathcal{V}_1))^{-2/d}} \left(\frac{b_n \lambda(\mathcal{V}_1)}{V(B_{b_n^{1/d}}(p))}\right)^{1/2}$, since $H6$ we obtain that $B_n \to \tau\ \beta^{(d+4)/d}/(6d+12)\ (f(p)\mu(\mathcal{V}_1))^{-2/d}$. A similar argument shows that $C_n \to 0$ and therefore we get that $w_n^{-1/2}(k_n - w_n) \to z + \beta^{\frac{d+4}{d}} \frac{\tau}{6d+12}(f(p)\lambda(\mathcal{V}_1))^{-d/2}$.

In order to concluded the proof we will show that $\dfrac{\mu_n}{w_n^{1/2}} \to \dfrac{\beta^{\frac{d+4}{d}}}{(f(p)\lambda(\mathcal{V}_1))^{(d+2)/d}} \displaystyle\int_{\mathcal{V}_1} u_1^2\ d\mathbf{u}\ L_1(p)$. We use a second Taylor expansion that leads to,

$$\int_{B_{b_n^{1/d}}(p)} (f(q) - f(p)) d\nu_g(q) = \sum_{i=1}^d \frac{\partial f \circ \psi^{-1}}{\partial u_i}|_{u=0} b_n^{1+1/d} \int_{\mathcal{V}_1} u_i\ \theta_p \circ \psi^{-1}(b_n^{1/d}\mathbf{u})\ d\mathbf{u}$$

$$+ \quad \sum_{i,j=1}^{d} \frac{\partial^2 f \circ \psi^{-1}}{\partial u_i \partial u_j}|_{u=0} b_n^{1+2/d} \int_{\mathcal{V}_1} u_i u_j \; \theta_p \circ \psi^{-1}(b_n^{1/d}\mathbf{u}) \; d\mathbf{u}$$
$$+ \quad O(b_n^{1+3/d}).$$

Using again a Taylor expansion on $\theta_p \circ \psi^{-1}(\cdot)$ at 0 we have that

$$\int_{B_{b_n^{1/d}}(p)} (f(q) - f(p)) d\nu_g(q) \quad = \quad b_n^{1+2/d} \int_{\mathcal{V}_1} u_1^2 \; d\mathbf{u} \; L_1(p) + O(b_n^{1+3/d})$$

and by $H6$ the theorem follows.□

References

[1] Bai, Z.D.; Rao, C. and Zhao, L. (1988). Kernel Estimators of Density Function of Directional Data. *J. Multivariate Anal.* **27,** 24-39.

[2] Boente, G. and Fraiman, R. (1991). Strong Order of Convergence and Asymptotic Distribution of Nearest Neighbor Density Estimates from Dependent Observations. *Sankhya: The Indian Journal of Statistics,* Series A, **53,** 2 194—205.

[3] Besse, A. (1978). Manifolds all of whose Geodesics are Closed. *Springer-Verlag.*

[4] Butler, R. (1992). Paleomagnetism:Magnetic Domains to Geologic Terranes.*Blackwell Scientific Publications.*

[5] Cox, A. and Doell, R. (1960). Review of Paleomagnetism, *Geol. Soc. Amer. Bull.* **71,** 645768.

[6] Devroye, L., and Wagner, T.J. (1977), The strong uniform consistency of nearest neighbor density estimates, *Annals of Statistics*,**3**, 536-540.

[7] Fisher, R. A. (1953). Dispersion on a sphere. *Proc. Roy. Soc. London, Ser. A* **217,** 295305.

[8] Fisher, N.I., T. Lewis, and B. J. J. Embleton (1987). Statistical Analysis of Spherical Data. *New York: Cambridge University Press.*

[9] Gallot, S., Hulin, D. and Lafontaine J. (2004) Riemannian Geometry. *Spriger. Third Edition.*

[10] García-Portugués, E; Crujeiras, R. and Gonzalez-Manteiga, W. (2011). Exploring wind direction and SO2 concentration by circularlinear density estimation. *Preprint.*

[11] Goh, A. and Vidal, R. (2008). Unsupervised Riemannian Clustering of Probability Density Functions. *Lecture Notes In Artificial Intelligence.* **5211.**

[12] Gray, A. and Vanhecke, L. (1979), Riemannian geometry as determined by the volumes of small geodesic balls, *Acta Math.*, 142, 157-198.

[13] Hall, P. , Watson, G.S. and Cabrera, J. (1987). Kernel density estimation with spherical data. *Biometrika* **74**, 751762.

[14] Henry, G. and Rodriguez, D. (2009). Kernel Density Estimation on Riemannian Manifolds: Asymptotic Results. *Journal Math. Imaging Vis.* **43,** 235-639.

[15] Jammalamadaka, S. and SenGupta, A. (2001). Topics in Circular Statistics. *Multivariate Analysis,***5**. World Scientific, Singapore.

[16] Joshi, J., Srivastava, A. and Jermyn, I. H. (2007). Riemannian Analysis of Probability Density Functions with Applications in Vision. *Proc. IEEE Computer Vision and Pattern Recognition.*

[17] Love, J. and Constable, C. (2003). Gaussian statistics for palaeomagnetic vectors. *Geophys. J. Int.* **152**, 515565.

[18] Mardia, K., and Jupp, P. (2000). Directional Data, *New York: Wiley*.

[19] Mardia, K. and Sutton, T. (1978). A Model for Cylindrical Variables with Applications. *Journal of the Royal Statistical Society. Series B. (Methodological),***40,**229-233.

[20] Parzen, E. (1962). On estimation of a probability density function and mode. *Ann. Math. Statist.* **33**, 1065–1076.

[21] Pelletier, B. (2005). Kernel Density Estimation on Riemannian Manifolds. *Statistics and Probability Letters*, **73, 3**, 297-304.

[22] Pennec, X. (2006). Intrinsic Statistics on Riemannian Manifolds: Basic Tools for Geometric Measurements. *Journal Math. Imaging Vis.*, **25,** 127-154.

[23] Rosenblatt, M. (1956). Remarks on some nonparametric estimates of a density function. *Ann. Math. Statist.***27**, 832–837

[24] Silverman, B.W. (1986) Density Estimation for Statistics and Data Analysis, Chapman & Hall.

[25] Wagner, T. (1975). Nonparametric estimates of probability densities. *IEEE Trans. Information Theory IT.* **21**, 438–440.